



1 **Identification of optimal ERA5 model level for wind 2 resource assessments in mountainous terrain**

3 Juan Contreras^{1,2}, Nicole van Lipzig², Esteban Samaniego³, and Daniela Ballari¹

4 ¹Instituto de Estudios de Régimen Seccional del Ecuador (IERSE), Universidad del Azuay, Cuenca,
5 010204, Ecuador

6 ²Department of Earth and Environmental Sciences, KU Leuven, Leuven, 3001, Belgium

7 ³Facultad de Ingeniería, Universidad de Cuenca, Cuenca, 010150, Ecuador

8

9 *Correspondence to:* Juan Contreras (juan.contreras@uazuay.edu.ec)

10 **Abstract.** Accurate estimation of hub-height wind speed is crucial for wind resources assessment at
11 prospective sites. Traditionally, long-term wind speed series are derived from short-term site observations
12 combined with reanalysis products, most commonly the ERA5 single-level data at 10 m and 100 m heights.
13 However, the coarse spatial resolution of ERA5 limits their reliability in complex mountainous regions,
14 leading to weak correlations with local wind measurements due to not adequately resolved near-surface
15 flow. This study investigates whether the use of wind speed estimates from upper atmospheric levels (i.e.,
16 model levels) of ERA5 model level data set can improve wind speed representation in complex terrain. We
17 compared ERA5 with hourly wind speed observations at 80 m from four meteorological masts located at
18 high elevations (2829–3796 m a.s.l.) in the tropical Andes of southern Ecuador, and developed site-specific
19 Random Forest (RF) models for calibrate ERA5 wind speeds. Our findings reveal that wind speeds from
20 upper model levels (~ 1000 – 1500 m for most of the sites) exhibit substantially stronger correlations with
21 mast observations than the theoretical hub-height. Compared with single-level inputs, model-level-driven
22 RF estimates achieved average improvements of 59% in Perkins Skill Score (PSS), 40% in R^2 , and 23% in
23 MAE/RMSE. Importantly, the bias in annual energy production (AEP) decreased to less than 7%, in
24 contrast with 22% when using ERA5 single-level data. These improvements were greater for sites located
25 on exposed peaks, which are often preferred locations for wind farms, where the local flow is better captured
26 by upper model levels. Overall, our results demonstrate that selecting appropriate upper ERA5 model levels
27 offers a cost-effective strategy to generate accurate, site-specific hub-height wind speed time series in
28 complex terrain. We encourage the wind energy community to exploit these upper atmospheric levels of
29 ERA5 to enhance wind resource assessments in mountainous regions.

30 **1. Introduction**

31 Understanding long-term wind speed at turbine height is essential for the wind energy industry, particularly
32 for site assessment and energy yield estimation (Watson, 2023). Direct in-situ measurements from
33 meteorological masts remain the gold standard for assessing wind resources at onshore locations (McKenna
34 et al., 2022; Watson, 2023). However, due to the high costs associated with deploying this infrastructure
35 and the urgent demand for wind energy development, these measurement campaigns typically span only 1–
36 2 years. Such short-term datasets are insufficient to capture the long-term wind conditions needed for
37 accurate wind resource assessment over a project's lifetime (Basse et al., 2021). To overcome this limitation,
38 the Measure–Correlate–Predict (MCP) methodology is widely used to extrapolate short-term wind speed
39 records. MCP involves correlating measurements at the candidate site with long-term data from nearby
40 reference sites, typically using linear regression techniques (Carta et al., 2013; Houndekindo & Ouarda,
41 2025b). In recent years, MCP methods have evolved to incorporate machine learning approaches for
42 building transfer functions and have increasingly relied on wind data from Numerical Weather Prediction
43 (NWP) models as reference sources, especially in areas lacking in-situ measurements (e.g., meteorological
44 masts or weather stations) (Houndekindo & Ouarda, 2025b).

45 Data from NWP models, particularly mesoscale simulations and global reanalysis datasets—have become
46 increasingly common as reference sources in MCP applications (Houndekindo & Ouarda, 2025b). Although
47 mesoscale models offer higher spatial and temporal resolution than global reanalyses, they are available
48 only for limited areas worldwide and typically cover less than 20 years (Borgers et al., 2024). This constrain
49 is primarily due to the substantial computational resources required to run these models, limiting their utility
50 for most parts of the world (McKenna et al., 2022). In contrast, reanalysis although with a coarser spatial



51 and temporal resolution than mesoscale models, it provides a global coverage making it useful in remote
52 areas (i.e., non-historical monitoring sites). Moreover, they often span multiple decades (e.g., 40 to 100
53 years) making them suitable for long-term resources assessments. Among these, the fifth generation
54 European Centre for Medium-Range Weather Forecasts atmospheric reanalysis system (ERA5) is the
55 preferred reanalysis in the wind power meteorology community (Olauson, 2018). Studies by Ramon et al.
56 (2019) and Gualtieri (2022) highlight its superior accuracy, reduced uncertainty, and greater reliability
57 compared to other global reanalysis datasets.

58 Although ERA5 wind speed data is sufficiently reliable on offshore and flat areas, significant discrepancies
59 are observed in mountainous regions. It is well-known that ERA5 tends to underestimate wind speeds—
60 and thus wind power potential—in these complex terrains (Gualtieri, 2022). Additionally, the temporal
61 variability of wind is reproduced less accurately compared to flat or offshore locations. These inaccuracies
62 are largely attributed to ERA5's coarse spatial resolution, which fails to capture the intricate topography
63 and surface roughness of mountainous areas. Grid-averaged winds in such regions often overlook speed-
64 up effects induced by terrain features (Gualtieri, 2022). In offshore and flat locations, several studies have
65 attempted to improve the MCP estimates incorporating physically-based covariates from ERA5 and data
66 from mesoscale models using machine learning methods, particularly random forest (e.g., Bodini et al.,
67 2023; Hallgren et al., 2024; Liu et al., 2023; Rouholahnejad & Gottschall, 2025; Schwegmann et al., 2023).
68 Conversely, in mountainous areas, research in this regard is extremely limited. One notable exception is the
69 study by Cavaiolà et al. (2023), who developed a random forest model using physics-based ERA5 variables
70 related to wind speed to estimate long-term wind power in the Alpine region. Besides, the above-mentioned
71 studies incorporated additional meteorological or physical variables, all of them pointed out wind speed as
72 the most critical predictor. Therefore, efforts to obtain accurate wind speed are of most relevance.

73 Expanding wind energy capacity, besides being strategic worldwide, is especially relevant in regions with
74 a low diversified energy matrix. This is the case of Ecuador, which although having considerable wind
75 resource potential in the Andes mountains, yet wind power currently accounts for only 0.6% of national
76 electricity production (Godoy et al., 2025), revealing a largely untapped opportunity for renewable energy
77 diversification. Additionally, the severe droughts experienced in 2023 and 2024 further exposed the
78 vulnerability of Ecuador's electricity sector, which remains highly dependent on hydropower (Tapia et al.,
79 2026). Expanding wind energy capacity is therefore strategic not only for diversifying the national energy
80 matrix and increasing resilience during drought events, but also for supporting carbon-neutrality goals. In
81 light of these challenges, there is an urgent need for robust wind resource assessment studies to guide future
82 development. However, most potential wind farm locations in the region are situated in complex
83 mountainous terrain, where reanalysis-based wind resource estimates remain highly uncertain.

84 Martinez et al. (2024) highlighted that global and regional reanalysis tend to underestimate actual site
85 elevations due to the smoothed representation of orography in the Andes. It is known that NWP models
86 (which form the basis of reanalysis datasets) are highly sensitive to lower boundary conditions (Hahmann
87 et al., 2020). The degree of topographic smoothing negatively affects their ability to simulate terrain-
88 induced wind phenomena such as anabatic and katabatic flows, mountain waves, and valley channelling
89 which are often lost in coarse-resolution models (Kumar et al., 2025). Recent findings by Pauscher et al.
90 (2024) indicate that reanalysis products tend to underestimate wind speeds at sites located above the grid-
91 cell mean elevation and overestimate them at sites below it in complex terrain. This raises the question of
92 whether wind speed estimates from reanalysis at elevations higher than the traditionally used levels (i.e.,
93 10 m and 100 m) could provide a better match with observations in mountainous areas.

94 Our hypothesis is that, in mountainous regions, wind speed from upper model level in ERA5 are more
95 representative of conditions at wind farm sites, as these locations are often exposed to free-atmospheric
96 flow rather than surface-level wind dynamics. It is important to highlight that ERA5 single level dataset
97 (10 m and 100 m wind components above the ground) has been established as a standard dataset in this field.
98 Thus, wind speed from ERA5 single level data has been commonly used as input data for MCP studies both
99 offshore and onshore. However, ERA5 model level dataset also provides more detailed vertical resolution
100 data in the atmosphere (i.e., 137 model level heights) which may be more relevant for a detailed wind
101 energy assessment. Note that this dataset has only been used in few studies, particularly at offshore locations
102 due to the higher height of wind turbines in comparison to onshore sites (e.g., Brune et al., 2021; Cheynet et
103 al., 2025; Hahmann et al., 2022; Hallgren et al., 2024; Soares et al., 2020). Given the mismatch between



104 the orography represented in reanalysis data and the actual terrain of mountainous sites, utilizing higher-
105 altitude wind speed data from ERA5 may be crucial for improving wind speed estimations in these areas.

106 Therefore, the aim of this study is to evaluate whether the use of higher atmospheric levels from ERA5
107 model level dataset can improve wind speed estimates and provide a more reliable time series for wind
108 resource assessment in the mountainous regions. Our study area is the tropical Andes of southern Ecuador
109 between 2829 and 3796 m a.s.l. To this end, we first analysed the relationship between observed wind speed
110 time series at hub height (80 m) and ERA5 wind speed estimates across various model levels, ranging from
111 10 m to approximately 3200 m above ground level, in order to identify the model level that best represents
112 wind conditions at the study sites. Next, we developed a random forest model to calibrate ERA5 and predict
113 wind speed estimates, using the optimal model height of wind speed from the model level dataset and
114 comparing against a reference model composed with the single level wind speed dataset. Finally, we
115 assessed the impact of these calibrated wind speed estimates on annual energy production (AEP), applying
116 power curves from existing wind farms in Ecuador. The findings of this study provide valuable insights for
117 improving wind speed estimation for wind resources assessment in complex terrains using reanalysis
118 datasets.

119 The structure of the paper is as follows: Section 2 describes the datasets and methodology; Section 3
120 presents the results; Section 4 discusses the findings; and Section 5 concludes the study with a summary
121 and final remarks.

122
123 **2. Materials and methods**
124

125 **2.1. Study area and in-situ masts**

126 Our study area is located in the Andes of southern Ecuador, spanning the provinces of Cañar, Azuay, and
127 El Oro (Fig. 1). The region is characterized by complex topography and heterogeneous land cover. High
128 wind power potential has been identified in areas situated above 2000 meters above sea level (m a.s.l.),
129 primarily along the ridges of the Andean Cordillera, near the Continental Divide of the Americas. This wind
130 potential has led to the planning of several wind farm projects in the region, including the construction of
131 Ecuador's largest operating wind farm, Minas de Huascachaca (57 MW).

132 The spatio-temporal variability of wind in the study area, and more broadly in the Andean region of
133 Ecuador, is influenced by both synoptic and valley-scale circulation patterns. At the seasonal scale, wind
134 patterns are primarily driven by the migration of the Intertropical Convergence Zone (ITCZ). The windy
135 season, which extends from June to September, corresponds to the northward migration of the ITCZ during
136 the boreal summer, strengthening the southern trade winds. Conversely, the calm season, from October to
137 May, is associated with the southward shift of the ITCZ over Ecuador (López et al., 2023). Throughout the
138 year, winds predominantly flow from the east and southeast, while westerly winds are more common during
139 the calm season, particularly at sites located closer to the lower western flanks of the Andes. At the daily
140 scale, thermally induced winds contribute to variability: anabatic winds occur during the day as heated air
141 rises along mountain slopes, while katabatic winds prevail at night as cooler air descends.

142 Wind observations were collected from four operational meteorological masts managed by the Electric
143 Corporation of Ecuador (CELEC EP): M1, M2, M3, and M4 (Fig. 1). M4, located in the northern part of
144 the study area, is predominantly surrounded by cattle grazing lands and croplands. M1 and M2, situated
145 centrally within the region, are representative of highland environments characterized by alpine grasslands
146 locally known as *páramo*. M3, in the southwest of the study area, is also surrounded by *páramo* and pine
147 forest. All masts are situated in wind exposed sites on ridges or hilltops.

148 The masts measure various meteorological variables; however, for this study, only wind speed data were
149 used. Each mast is equipped with four first-class cup anemometers (Thies CLIMA 4.331.10.000) measuring
150 wind speed at heights of 40, 60, 78, and 80 m above ground level, with readings recorded every 10 minutes.
151 For our analysis, wind speed measurements at the highest level (80 m) were used. To ensure consistency
152 between the temporal resolution of the ERA5 data and the mast observations, hourly wind speed averages
153 were computed from the 10-minute measurements. Only complete hours, defined as those with at least six



154 valid 10-minute measurements, were included to avoid uncertainties in the hourly calculations. The wind
 155 speed observations cover the period from January 1, 2021, to December 31, 2024.

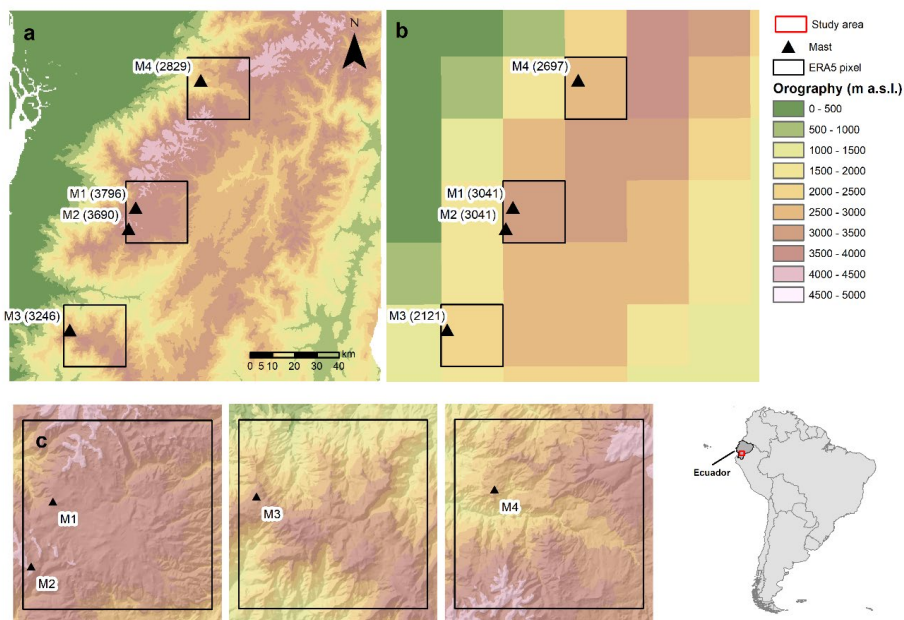
156 Wind speed data at 80 m underwent quality control, through detailed visual inspection and correlation
 157 analysis with wind speed measurements at the other heights, was done following MEASNET guidelines
 158 (MEASNET, 2022). Data from July 20, 2022, to September 8, 2022, at M2 were excluded due to sensor
 159 failure. Additional data gaps were identified, mainly related to maintenance campaigns and intermittent
 160 power outages caused by persistent cloudy conditions at the sites. Further details on data gaps and site
 161 characteristics are provided in Table 1.

162 **Table 1: Details of the study sites and data availability at 80 m during the study period. The terrain**
 163 **category was calculated using the standard deviation of elevation within a 10 km radius around each**
 164 **site based on the criteria of Borowski et al. (2025).**

Site	Elevation (m a.s.l.)	Land cover	Landform	SD Elevation (m a.s.l.)	Terrain category	Data availability (%)
M1	3796	Paramo	Ridge	471	Very complex	93.2
M2	3690	Paramo	Ridge	317	Very complex	83.4
M3	3246	Paramo/Pine Forest	Ridge	671	Very complex	99.6
M4	2829	Agriculture	Hilltop	536	Very complex	97.4

165

166



167

168 **Figure 1: Map of the study area and location of meteorological masts. The orography of the study**
 169 **region according to the Shuttle Radar Topography Mission (SRTM) digital elevation model (30 m)**
 170 **and the ERA5 (~31 km) is shown in (a) and (b), respectively. In parenthesis is the in-situ and ERA5**
 171 **elevation of sites in m a.s.l. The variability of orography inside the ERA5 pixel for each site is shown**
 172 **in (c). Grid coordinates were omitted from all maps for confidential proposes.**

173 **2.2. ERA5 data**



174 ERA5 is the fifth-generation reanalysis product developed by the European Centre for Medium-Range
175 Weather Forecasts (ECMWF). It combines numerical weather prediction models with historical
176 observational data using the Integrated Forecasting System (IFS) Cycle 41r2 assimilation model to provide
177 hourly atmospheric variables dating back to 1940 (Hersbach et al., 2020). The spatial resolution of the
178 ERA5 reanalysis dataset is approximately 31 km, with global coverage.

179 Two ERA5 datasets were used in this study: (1) ERA5 data on single levels, which provide wind
180 components at 10 m and 100 m above ground level, and (2) ERA5 data on model levels, which provide
181 wind components from the surface up to approximately 80 km altitude across 137 vertical levels. The first
182 dataset has been widely used for wind resource assessment and is considered a standard reference in the
183 wind energy industry, whereas ERA5 model level data have been less commonly applied in the literature.

184 A total of 33 model levels, ranging from 10 m (level 137 - L137) to approximately 3000 m (level 105 -
185 L105), were selected from the ERA5 model level dataset to evaluate their relationship with wind
186 observations. The wind components from both ERA5 datasets were downloaded using the Climate Data
187 Store API in Python. For each of the four mast locations, ERA5 data were extracted from the nearest grid
188 points without interpolation (see Fig. 1). This means that M1 and M2 masts have the same timeseries.
189 Finally, wind speed was calculated from the u and v wind components for both datasets.

190 **2.3. Evaluation and selection of optimal heights from ERA5 model level data**

191 Measure-Correlate-Predict (MCP) methods traditionally require a high degree of correlation between wind
192 speed observations and reference data (e.g., reanalysis datasets) to be considered suitable for wind speed
193 prediction. This is commonly assessed using the correlation coefficient (Carta et al., 2013). We used the
194 Pearson correlation coefficient to evaluate the relationship between wind speed measurements from the
195 meteorological masts and wind speeds from various ERA5 model levels (ranging from 10 m to 3000 m).
196 The model level height with the strongest correlation was then selected to estimate wind speed.

197 **2.4. Wind speed prediction**

198 Wind speed predictions were obtained using the Random Forest (RF) algorithm (Breiman, 2001). This
199 method has been widely used in recent years to estimate wind speed and wind energy production due to its
200 high flexibility and robustness. RF has demonstrated comparable results to other sophisticated machine
201 learning models (Abdelsattar et al., 2025), and is considered one of the most popular methods for wind
202 speed prediction (Houndekindo & Ouarda, 2025).

203 The RF algorithm builds an ensemble of individual decision trees. Each tree is constructed using a random
204 subset of the training data, which minimizes overfitting and ensures independent predictions. The final
205 prediction is computed as the average of the individual tree outputs. Additional details on the RF algorithm
206 can be found in Breiman (2001) and Gentleman and Poggi (2020).

207 In this study, the RF model was preferred over a conventional regression model because it provides more
208 consistent predictions (e.g., non-negative values), particularly at low wind speeds. Accordingly, the RF was
209 applied to estimate wind speed at 80 m for each site, using observed wind speed at this height as reference
210 data and ERA5 wind speed as predictors. Specifically, we trained two RF models: (1) RF1 - a model using
211 hourly wind speed at 10 m and 100 m from the ERA5 single-level dataset, and (2) RF2 - a model using
212 hourly wind speed at the height with the strongest correlation to mast measurements from the ERA5 model-
213 level dataset (identified in section 2.3). The first model serves as a benchmark to compare the differences
214 and potential improvements achieved by using the optimal model level height. It is important to note that,
215 although most studies commonly use either 10 m or 100 m ERA5 wind speed variables to estimate near-
216 surface wind speeds, we used both variables, as this combination explained a greater portion of variance in
217 the RF models than using a single variable alone (see Table. A1).

218 For each site, both models were trained using observed hourly wind speed data from the first three years of
219 the monitoring campaign (i.e., January 2021 to December 2023), and model performance was evaluated
220 using data from the last year (i.e., January 2024 to December 2024). Further details on the number of
221 samples used for training and testing for each site are provided in Table 2.

222 The number of trees and the minimum leaf size, which are the most important parameters of the RF model,
223 were set to 500 and 5, respectively. These values correspond to the recommended default settings of the



224 *randomForest* function in R (Breiman et al., 2025). Since the main objective of this study is to highlight
225 the improvements achieved by incorporating appropriate ERA5 wind speed heights, we did not conduct a
226 hyperparameter optimization for each site. This decision is further supported by the fact that some studies
227 have reported similar values for their optimal parameter settings (Hallgren et al., 2024; Liu et al., 2024).

228 **Table 2: Number of samples used for training period (2021-2023) and testing period (2024) for the**
229 **random forest models. Percentage of data available relative to each period is shown in parentheses.**

Site	Training period	Testing period
M1	23890 (90.9%)	8784 (100%)
M2	20458 (77.8%)	8784 (100%)
M3	26125 (99.4%)	8784 (100%)
M4	25904 (98.6%)	8237 (93.8%)

230

231 2.5. Performance evaluation metrics

232 In order to quantify the discrepancies between the wind speeds estimated by the RF models and the mast
233 wind speed data, three commonly used metrics were employed: root mean squared error (RMSE), mean
234 absolute error (MAE), and the coefficient of determination (R^2). The RMSE quantifies the average
235 magnitude of the errors and indicates how much the predictions deviate from the reference data. A higher
236 RMSE reflects larger deviations, as this metric gives greater weight to larger errors due to the quadratic
237 term. The MAE calculates the mean of the absolute differences between the reference values and the
238 predictions, treating larger and smaller errors equally without applying additional weighting. The R^2
239 coefficient measures the strength of the linear correlation between the observed and predicted wind speeds.
240 These metrics are defined as follows (Eqs. 1-3):

$$241 \quad RMSE = \sqrt{\frac{1}{n} \sum_{i=1}^n (y_i - \hat{y}_i)^2} \quad (1)$$

$$242 \quad MAE = \frac{1}{n} \sum_{i=1}^n |y_i - \hat{y}_i| \quad (2)$$

$$243 \quad R^2 = 1 - \frac{\sum_{i=1}^n (y_i - \hat{y}_i)^2}{\sum_{i=1}^n (y_i - \bar{y})^2} \quad (3)$$

244 where y_i and \hat{y}_i are the i th measured and the corresponding predicted values of wind speed. The average
245 of the measured wind speed values is denoted by \bar{y} . The total sample size in the test set is N .

246 In addition, the Perkins Score Skill test (PSS) was employed to quantifies the discrepancies in the frequency
247 distribution between estimated and observed wind speed using Eq. (4).

$$248 \quad PSS (H_1, H_2) = \sum_{b=1}^n MIN(F_{H_1}^b, F_{H_2}^b) \quad (4)$$

249 where H_1 and H_2 represents the first and second histogram and F^b represents the normalized frequency for
250 bin b . The PSS represents the fraction of overlap between the two histograms, so that a PSS of 1 represents
251 complete overlap while a value of 0 indicates a complete mismatch. The PSS was calculated considering a
252 detailed bin width of 1 m s^{-1} similar to Borgers et al. (2024).

253 2.6. Wind energy estimation and evaluation

254 This subsection outlines the methodology used to evaluate how wind speed data from different RF models
255 (i.e., using ERA5 single-level or model-level data) influence the estimated annual energy production (AEP)
256 at the four study sites. Two power curves were considered in the analysis, based on the turbines installed in
257 existing wind farms in continental Ecuador (Villonaco: 2700 m a.s.l. and Minas de Huascachaca: 1100 m
258 a.s.l.): the Goldwind GW70/1500 and the Vestas V112/3450. Although Minas de Huascachaca operates
259 with Dongfang Electric Corporation wind turbines, the corresponding power curves were not publicly
260 available. Therefore, we used the Vestas V112/3450 power curve, which has similar characteristics to the
261 turbines installed at that site. Details on the turbine operational ranges, hub heights, and the power curves
262 used in this study are provided in Table 3 and Fig. A2 (in Appendix section), respectively.



263 The AEP was calculated using wind speed estimates from the RF models at a hub height of 80 m. The
264 percentage error (PE) was used to quantify the differences in wind energy estimates based on the different
265 wind speed predictions. This evaluation was carried out for the year 2024 which was not part of the RF
266 training dataset. The PE was calculated using Eq. (5).

267

$$268 \quad PE = \frac{AEP_{RF} - AEP_{SYN}}{AEP_{RF}} \times 100\% \quad (5)$$

269

270 where AEP_{RF} is the annual energy production modelled from wind speed estimated by the RF models, and
271 AEP_{SYN} is the synthetic annual energy production modelled from observed wind speed data.

272

273 **Table 3: Details of the wind turbines considered in the study.**

Model	Power (MW)	Cut-in wind speed (m s ⁻¹)	Rated wind speed (m s ⁻¹)	Cut-off wind speed (m s ⁻¹)	Hub height range (m)	Rotor diameter (m)	Wind class
GW70/1500	1.5	2.5	14	25	65 - 100	70.3	IEC Ia/IIa1
V112/3450	3.45	4	12.5	25	69 - 94	112	IEC A

274

275 **3. Results**

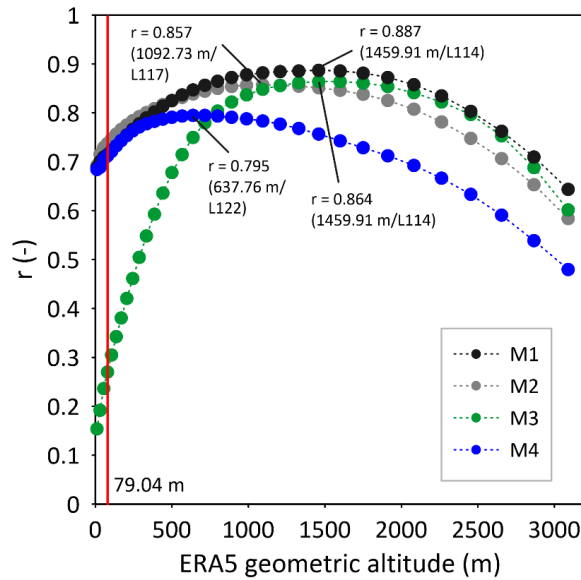
276

277 **3.1. Evaluation and selection of optimal heights from ERA5 model level data**

278 The correlation between wind speed observations and ERA5 model level data at different heights above
279 ground level (i.e. geometric altitude) is shown in Fig. 2. An inverted parabolic relationship is observed
280 between correlation magnitude and height: correlation values increase steadily from ~0.27 – 0.74 at hub-
281 height (79.04 m; the closest ERA5 model level height) until reaching a maximum of ~0.80 – 0.89, after
282 which the correlation begins to decrease. The maximum correlation between observations and ERA5 data
283 was consistently achieved at heights substantially higher (~600 - 1500 m) than the measurement height (80
284 m) across all mast locations. To corroborate our findings, we performed the same analysis at 3 sites with
285 flat topography in the Coast region of Ecuador (2 located at the coastline and 1 at inner location) (see Fig.
286 A1 in Appendix). The results showed that, at coastal and flat locations, the strongest correlations with
287 observed wind speeds occurred near the actual hub height (< 245 m), with little differences in the correlation
288 values between the closest level to the observations and the height of highest correlation ($r < 0.03$). In
289 addition, higher correlations between observations and ERA5 were observed for the inner site in
290 comparison of coastal sites. These results using ERA5 model level data indicates that wind speeds over flat
291 terrain is representative of hub-height conditions at coastal and inner flat sites but are not representative in
292 mountainous areas.



293



294

295 **Figure 2: Correlation between observed wind speed at four sites at 80 m height and ERA5 data at**
296 **different geometric altitudes for the period Jan-2021 to Dec 2024. The red line shows the closest model**
297 **height to the observations. The highest correlation value and their respective altitude and model level**
(in parenthesis) are indicated for each site.

298

299 Notably, at M3, the correlation increased from approximately 0.27 at the measurement hub height to 0.86
300 at the height of maximum correlation, underscoring the potential for improving wind speed estimates by
301 identifying optimal model heights. This pronounced difference, compared to the other sites, may be
302 attributed to the larger discrepancy between the actual site elevation and the ERA5 model elevation. The
303 height of maximum correlation was similar for M1, M3, and M2, while for M4 it occurred at a lower
304 elevation. Interestingly, the magnitude of the maximum correlation was comparable for M1 (0.887), M2
305 (0.857), and M3 (0.864)—all of which are located on well exposed areas—but was lower for M4 (0.795),
306 which is situated around hills probably influencing local wind speed behaviour (see Fig. 1c).

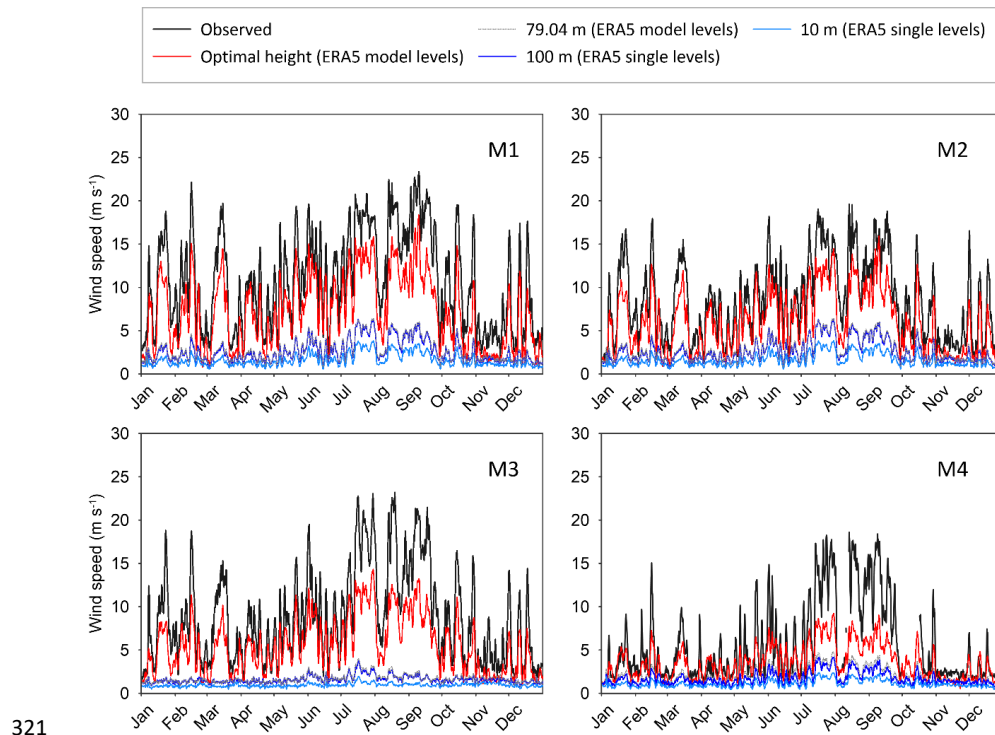
307

308 Figure 3 shows the comparison between hourly wind speed time series for the year 2024 for all ERA5
309 datasets and the observations. The ERA5 datasets include wind speeds at 10 m and 100 m, as well as wind
310 speeds at the closest height to the observations (79.04 m) and at the optimal correlation heights identified
311 in Fig. 2, both extracted from the ERA5 single level and model level dataset, respectively. Fig 3. shows
312 substantial discrepancies between observed wind speeds and those estimated using ERA5 single level data
313 (at 10 and 100 m). The wind speed from the model level data at the height closest to the observations shows
314 similar variability and magnitude to the ERA5 single level data at 100 m showing a systematic
315 underestimation around the year.

316

317 In contrast, the wind speed time series retrieved using the optimal correlation heights demonstrated
318 substantial improvements in representing wind speed variability across all study sites, although wind speeds
319 were still underestimated particularly during high wind periods. The dynamics of wind speed were better
320 captured at the M1 and M2 sites compared to the others. This analysis clearly suggests the potential for
321 improving wind speed estimates by using higher model level heights from ERA5 as reference data for MCP
322 modelling.

323



321
322 **Figure 3: Wind speed time series for the observations and ERA5 data in 2024. The times series shows**
323 **the 24 h running average instead of the hourly time series for visualization proposes. Note that at M1,**
324 **M2 and M3, the wind speed series at 100 m (ERA5 single level) and 79.04 m (ERA5 model level)**
325 **overlap.**

326

327 3.2. Evaluation of wind speed predictions

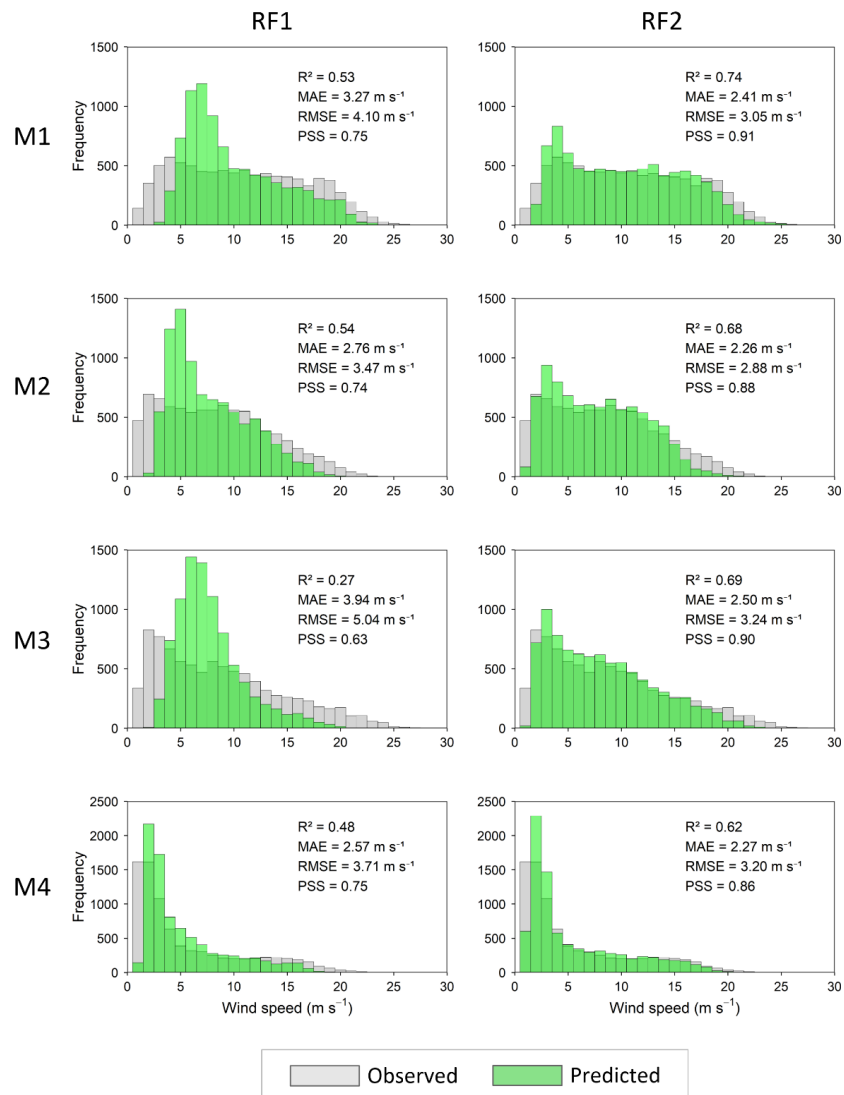
328 The frequency distributions of observed and predicted wind speed is shown in Fig. 4 along with their
329 evaluation metrics for the validation period (year 2024). A clear difference is observed in the measured
330 wind speed distribution of M1, M2 and M3 compared to M4 where high frequency of low wind speed
331 values ($<2 \text{ m s}^{-1}$) is frequent in comparison to the other sites.

332 The optimal model height as input for wind speed prediction (i.e., RF2 model) provided the best match with
333 the observed data for all sites, leading to a higher R^2 and PSS performances and lower MAE and RMSE
334 values than the predictions that use ERA5 single level data (i.e., RF1 model). The average values of the
335 four sites show an improvement of 40% in R^2 values while for MAE and RMSE led an improvement of
336 23% in both metrics. For PSS, the predictions reach an improvement of 59% respect to the reference model.
337 These results indicate a higher improvement in the predictions to simulate the wind speed dynamics and
338 distribution than the magnitude of wind speed.

339 The wind speed predictions of RF1 showed moderate similarity for all sites, with PSS values ranging from
340 0.75 to 0.74 at M1, M2 and M4 and 0.63 at M3. At M1, M2 and M3 it was observed an underestimation of
341 extreme wind speed values (low and high) and the overestimation of middle range values (from 4-9 m s^{-1}).
342 The RF2 predictions specially overcome these high discrepancies of middle range wind speed values
343 increasing the PSS above 0.86 for all sites, indicating its superior capability to replicate the observed wind
344 speed distributions. The improvement is especially remarkable at M3, where the PSS increases from 0.63
345 in RF1 to 0.90 in RF2.



346 Despite the improved performance with RF2 model, systematic discrepancies remain. In general, the
347 modelled distributions tended to underestimate the frequency of very low wind speeds (i.e., $<1 \text{ m s}^{-1}$) and
348 overestimated the frequency of moderate wind speeds, particularly at M2 and M3. In addition, the frequency
349 of high wind speeds ($>15 \text{ m s}^{-1}$) was underestimated for all sites, especially at M1, M2 and M3. These
350 ranges, however, varied slightly by site (Fig. 4). These biases suggested yet challenges in capturing the full
351 variability of wind speeds, particularly at the distribution extremes.



352

353 **Figure 4: Comparison of wind speed frequency distributions between observed wind speeds and**
354 **predictions from two Random Forest (RF) models across the four study sites for the year 2024. The**
355 **left column (RF1) shows results using ERA5 wind speeds at 10 m and 100 m (single-level dataset),**
356 **while the right column (RF2) shows results using ERA5 wind speed at the optimal model level height**
357 **identified through correlation analysis. For each site, the figure also displays the performance**
358 **metrics.**

359 **3.3. Annual wind energy estimation**



360 The results presented in Table 4 show the annual energy production (AEP) estimates obtained using the
361 Random Forest models compared to the observed AEP values for different turbine types at the four study
362 sites. Overall, predictions using the optimal wind speed height (RF2 model) consistently outperformed the
363 estimates based on ERA5 single level data (RF1 model), providing lower percentage errors across all
364 locations and turbine types.

365 The percentage error (PE) for RF2 was reduced by approximately a factor of three compared to the reference
366 model (RF1) for both turbines, indicating substantial improvements in AEP estimation accuracy. The
367 similar PE values obtained using the two different power curves suggest that the choice of power curve had
368 little influence on the relative accuracy of the AEP estimates in this case.

369 The RF2 model achieved the smallest discrepancies at the highest elevation site (M1), with PE values of -
370 1.99% for the GW70/1500 turbine and -2.11% for the V112/3450 turbine. In contrast, the largest deviations
371 were observed at M2, where the PE reached approximately 7%.

372 These findings highlight the importance of using appropriate ERA5 model level heights for improving wind
373 energy production estimates in complex mountainous environments.

374 **Table 4: Annual Energy Production (AEP) estimates from various wind speed Random Forest models**
375 **compared with observed data. The best-performing models, showing the smallest discrepancies, are**
376 **highlighted in bold.**

Location	Turbine	AEP (MWh)	PE (%)	
			RF1	RF2
M1	GW70/1500	7787.97	-7.71	-1.99
	V112/3450	18059.60	-7.78	-2.11
M2	GW70/1500	6097.76	-16.35	-7.06
	V112/3450	14221.59	-17.60	-7.14
M3	GW70/1500	6059.96	-20.78	-5.72
	V112/3450	14063.40	-21.63	-5.77
M4	GW70/1500	3137.02	-18.83	-4.20
	V112/3450	7180.74	-20.02	-4.18

377

378

379 **4. Discussion**

380 Our study evaluated the hypothesis that, in the Andean mountainous region, wind speed from higher model
381 levels in ERA5 are more representative of conditions at wind farm sites than the traditionally used 10 or
382 100 m single level ERA5, as these locations are often exposed to free-atmospheric flow rather than surface-
383 level wind dynamics. Even if the topographic issue in mountain areas was previously identified in the
384 literature (Gualtieri, 2022), this is the first time that higher model level heights were explored, identifying
385 its suitability.

386 The results presented above confirms that ERA5 consistently underestimates wind speed variability in the
387 tropical Andes in line with other studies in complex terrain (e.g., Draeger et al., 2024; Hu et al., 2023;
388 Jourdier, 2020; Khadka et al., 2022). A central result, in line with our hypothesis, is that higher atmospheric
389 levels of ERA5 (i.e., from model levels dataset) above the hub-height are stronger correlated to observed
390 wind speed than lower levels at the hub-heights. This is not the case for coastal masts where higher
391 correlations between ERA5 and observed wind speed were very close to the hub-heights (Fig. A1).
392 Although in both Pacific coast and Andean regions, the highest correlation is above the hub-height of 80
393 m, these differences are significantly amplified for Andean sites. Therefore, these results support our
394 hypothesis that observed wind speed in the Andes is more closely tied to upper atmospheric levels of ERA5
395 than to surface-level data.

396 Interestingly, optimal heights in the Andes were higher when differences between in-situ measured and
397 ERA5 topography were larger too. This pattern may be explained by the coarse spatial terrain representation



398 of ERA5, which smooths the intricated terrain features within each grid cell, simulating lower wind speeds.
399 For instance, the highest improvement in the level of correlation between hub height and the optimal level
400 height was achieved particularly in M3 where differences in topography were strong. In this particular case,
401 M3 is located at a peak compared to most of the surrounding landscape area within the ERA5 grid (Fig.
402 1c). These results highlight the possibility to estimate wind speed using ERA5 wind speed for a particular
403 site by selecting higher model level heights.

404 A substantial improvement in the prediction of wind speed was obtained using optimal height information
405 of ERA5 model levels in comparison with the commonly used 10 m and 100 m wind speed heights of ERA5
406 single levels, corroborating the suitability of using this specific dataset for mountain areas. Wind speed
407 estimation showed similar performance for all sites using the optimal heights of ERA5 model levels
408 compared to the ERA5 single level datasets; however, relatively small differences were noticed at M4. The
409 lower performance in M4 is caused by the lower performance of the RF models in estimating particularly
410 lower wind speeds (i.e., $0\text{--}2 \text{ m s}^{-1}$) where high frequency values within this range are common in this site.

411 Comparing our findings with previous studies in a strictly fair way is challenging because two main reasons:
412 (i) most studies considered other covariates in the predictive models or/and (ii) include wind speed
413 observations at surface level (e.g., meteorological stations) as input variables in the predictive models. It is
414 expected that for both aforementioned cases better wind speed estimates would be achieved compared to
415 our study that use only a single variable from reanalysis data in comparison to a model that use local
416 information (e.g., observed wind speed generally at 2 m or 10 m). However, despite the limited input
417 features included in our model (i.e., a single height of wind speed) and the source of its information (i.e.,
418 ERA5 reanalysis), our results were comparable in terms of performance with previous studies
419 (Houndekindo & Ouarda, 2025a; Hu et al., 2023; Liu et al., 2023). Liu et al. (2023) used a RF model to
420 estimate wind speed at several hub-heights using measured wind speed at 10 m (anemometer) and 300 m
421 (radar wind profiler) and ERA5 covariates as input features for a coastal location in China. Hu et al. (2023)
422 used the eXtreme gradient boosting (XGBoost) algorithm using topographical position index and ERA5
423 variables to predict wind speed at 10 m over Europe.

424 Our estimates were also comparable with the outcomes of more sophisticated machine learning algorithms.
425 For instance, Houndekindo & Ouarda (2025a) used a long short-term memory (LSTM) and transformers
426 models to bias correct ERA5 hourly wind speeds for WRA. The models outperformed static bias correction
427 approaches and other machine learning methods. Particularly at hilly and mountainous sites, median values
428 of the testing sites shown an $r = 0.79$. This performance is similar to that of our study, where M1 ($r = 0.86$),
429 M2 ($r = 0.82$) and M3 ($r = 0.83$) showed even larger r values. In addition, the distribution of wind speed
430 was better estimated with our approach showing higher values of PSS (PSS $> 75\%$ or 0.75). It is important
431 to note that Houndekindo and Ouarda (2025) included time-resolved covariates (e.g., 10 m u- and 10 m v-
432 components, 10 m wind speed, 2 m temperature, boundary layer height, and surface pressure) and several
433 static covariates (derived from a Digital Elevation Model and land cover maps) in their model. All these
434 comparisons highlight the competitiveness of our parsimonious approach for a local site estimation of wind
435 speed in complex mountainous areas.

436 The study of the impact of wind estimates on energy production is not commonly assed in previous studies.
437 The higher improvement in the reduction of underestimation of AEP estimates is promising for the
438 evaluation of annual production. The best AEP estimates in M1 in comparison to the other sites are related
439 to the lower occurrence of low wind speed which all the sites poorly estimate as was indicated previously.
440 The impact of standard power curves used in this study shown negligible influence on the AEP estimation
441 in our study area. This is because the cut-in wind speed of turbines considered in the study are above 2-4
442 m s^{-1} , being discarded values below this threshold in the calculation of AEP. This result indicates that wind
443 speed estimates obtained by our approach could be reliable for the estimation of AEP using different turbine
444 models. However, higher underestimations would be expected for sites with high frequencies of low wind
445 speed.

446 It should be noted that as our main objective was to highlight the suitability of an optimal model level height
447 to estimate wind speed, no other heights were included in the RF model. Further studies could consider
448 additional closest level heights to the optimal level as input features to improve the wind speed estimates.
449 We expect that the inclusion of these levels might improve the representation of interactions between
450 atmospheric heights as they emulate wind shear effects as was evidenced using 10 m and 100 m ERA5



451 wind speed in the reference model. In addition, due to the highly complex topography interactions in the
452 Andes, sub-grid scale variables from ERA5 representing surface-atmosphere interactions could be tested
453 to improve wind speed estimates. Particularly, gravity waves have been identified as a relevant variable to
454 estimate wind speed in mountainous areas (e.g., Hu et al., 2023). We are also aware that optimal heights
455 were obtained after a detailed search of candidate heights which may require analyse relatively large
456 amounts of information. Thus, future studies are necessary to include more masts sites to identify
457 relationships between the performance of ERA5 and differences in topographical features as a practical
458 model for the search of optimal levels for sites.

459 Anticipating the impacts of climate change on the future energy yield of wind farm projects is essential for
460 strategic planning in the wind industry. A common approach is to directly analyse Global Climate Model
461 (GCM) projections (e.g., Devis et al., 2018; Hahmann et al., 2022; A. Martinez & Iglesias, 2024). However,
462 the coarse spatial resolution of GCM data (typically ≥ 100 km grid spacing) limits their suitability to regional
463 or global-scale assessments. Further studies could explore the use of higher atmospheric model levels from
464 GCMs to support downscaling of wind speed projections to local scales in mountainous regions, without
465 the need for computationally expensive full dynamical downscaling. Alternatively, a hybrid statistical-
466 dynamical framework, such as the approach proposed by Borgers et al. (2025), which integrates mesoscale
467 model output with GCM projections, could offer a promising solution for producing reliable local-scale
468 wind speed projections in complex terrain and prospective wind farm sites.

469 **5. Conclusions**

470 This study examined whether the use of higher atmospheric levels from the ERA5 model-level dataset can
471 improve wind speed predictions compared to the conventional use of ERA5 single-level data in the complex
472 mountainous terrain of the tropical Andes. Site-specific Random Forest (RF) models were trained using
473 three years of hourly wind speed observations at 80 m from four high-altitude masts located in southern
474 Ecuador. The predictions were validated against an independent year of observations and further tested for
475 energy applications through the estimation of annual energy production (AEP) using two representative
476 power curves.

477 The results demonstrate that wind speeds from higher ERA5 model levels (i.e., levels above ~ 1000 m for
478 most sites) show stronger correlations with observed wind speeds than the conventional single-level data
479 at 10 m and 100 m. Consequently, the ERA5 model level with the highest correlation proved more suitable
480 for wind speed prediction. Improvements were most pronounced at well-exposed sites located on peaks,
481 while localized sites with surrounding obstacles (e.g., M4) showed smaller gains. Predictions captured wind
482 speed variability and distribution more effectively than absolute magnitudes (i.e., RMSE). For energy
483 applications, the percentage error in AEP was significantly reduced to $\sim 2\text{--}7\%$ compared with $\sim 8\text{--}22\%$ when
484 using ERA5 single level data.

485 These findings highlight the potential of combining higher ERA5 model level data with Random Forest
486 models as a powerful and cost-effective approach for wind resource assessment in mountainous areas. Since
487 this method relies on freely available reanalysis data and requires relatively low computational cost, it
488 provides a practical alternative to mesoscale climate models for estimating long-term site-specific wind
489 speed and energy production in complex terrain.

490 **Appendices**

491 **Table A1: Percentage of explained variance of Random Forest models trained using various
492 combinations of ERA5 single level wind speed inputs. In bold the best model for each site.**

Input	M1	M2	M3	M4
10 m	34.02	36.01	-30.99	21.89
100 m	33.97	39.58	-16.42	31.07
10 m + 100 m	48.04	50.45	21.78	48.84

493

494



495

496

497

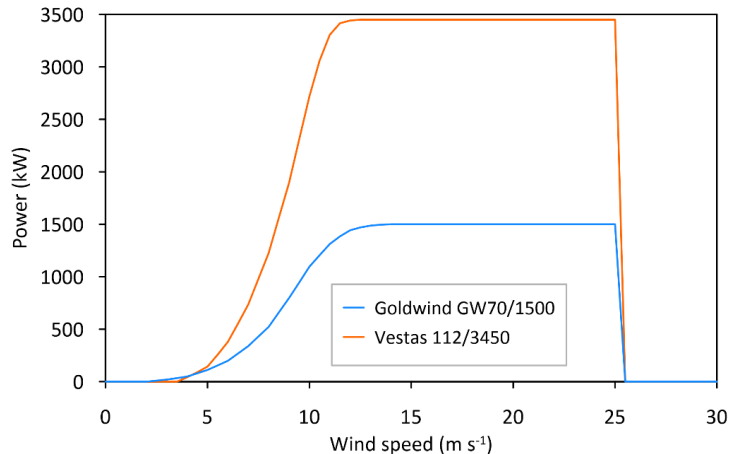
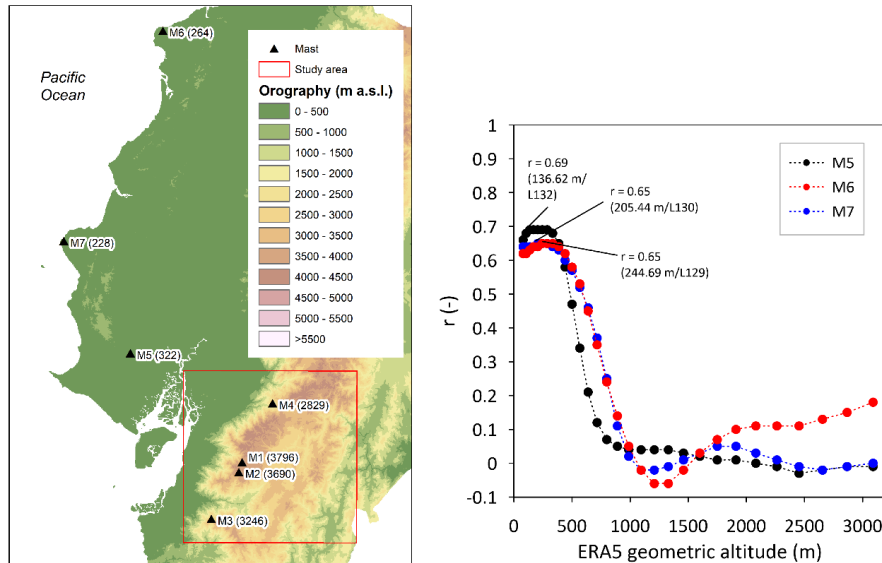


Figure A1: Power curves of the two reference turbines employed in this study.



498

499 Figure A2: Correlation between observed wind speed at four Coast sites at 80 m height and ERA5
500 data at different geometric altitudes for the period Jan-2021 to Dec 2024. In the left side, the map
501 shows, in parentheses, the actual elevation of each site (m a.s.l.). In the right side, the highest
502 correlation value and their respective altitude and model level (in parenthesis) are indicated for each
503 site.

504

505



506 **Code availability.** The codes used for download data and analyses presented in this study are available
507 upon request to the main author.

508 **Data availability.** Data from meteorological masts used in this research is not publicly accessible due to
509 proprietary restrictions and confidentiality agreements.

510 **Author contribution.** JC: conceptualization, data curation, formal analysis, investigation, methodology,
511 software, visualisation, writing (original draft preparation, review and editing); NvL: conceptualization,
512 methodology, writing (review and editing), supervision; ES: writing (review and editing), supervision; DB:
513 methodology, writing (review and editing), supervision, resources, funding acquisition.

514 **Competing interests.** The authors declare that they have no conflict of interest.

515 **Acknowledgements.** The authors are especially grateful to CELEC for providing wind observation mast
516 data through the inter-institutional agreement "Spatio-temporal applications supporting decision-making
517 for renewable energy and climate change – CSR-CON-0058-23". This research was supported by
518 Universidad del Azuay under the project "Wind energy resources in a context of change: spatio-temporal
519 dynamics and future projections for renewable energies in areas of high topographic complexity", grant
520 number 2023-0178. This study is an outcome of the joint PhD agreement between the Natural Renewable
521 Resources Doctoral Program offered by Universidad de Cuenca and Universidad del Azuay, and the
522 Doctoral Program in Science offered by KU Leuven.

523 **References**

524 Abdelsattar, M., Ismeil, M. A., Menoufi, K., Moety, A. A., & Emad-Eldeen, A. (2025). Evaluating
525 Machine Learning and Deep Learning models for predicting Wind Turbine power output from
526 environmental factors. *PLoS ONE*, 20(20). <https://doi.org/10.1371/journal.pone.0317619>

527 Basse, A., Callies, D., Grötzner, A., & Pauscher, L. (2021). Seasonal effects in the long-term correction of
528 short-term wind measurements using reanalysis data. *Wind Energy Science*, 6, 1473–1490.
529 <https://doi.org/10.5194/wes-6-1473-2021>

530 Bodini, N., Castagneri, S., & Optis, M. (2023). Long-term uncertainty quantification in WRF-modeled
531 offshore wind resource off the US Atlantic coast. *Wind Energy Science*, 8(4), 607–620.
532 <https://doi.org/10.5194/wes-8-607-2023>

533 Borgers, R., Dirksen, M., Wijnant, I. L., Stepek, A., Stoffelen, A., Akhtar, N., Neirynck, J., Van De Walle,
534 J., Meyers, J., & Van Lipzig, N. P. M. (2024). Mesoscale modelling of North Sea wind resources
535 with COSMO-CLM: model evaluation and impact assessment of future wind farm characteristics
536 on cluster-scale wake losses. *Wind Energy Science*, 9(3), 697–719. <https://doi.org/10.5194/wes-9-697-2024>

538 Borgers, R., Pinto, J. G., & Lipzig, N. Van. (2025). Quantifying the Near-Future Wind Energy Production
539 over the North Sea Using a Novel Statistical-Dynamical Approach to GCM Downscaling. *Journal*
540 *of Applied Meteorology and Climatology*, 365–381. <https://doi.org/10.1175/JAMC-D-24-0116.1>

542 Breiman, L. (2001). Random Forests. *Machine Learning*, 45, 5–32.

543 Breiman, L., Cutler, A., Liaw, A., & Wiener, M. (2025). Package ‘randomForest.’ In *Machine Learning*
544 (Vol. 45, Issue 1). <https://doi.org/10.1023/A:1010933404324>

545 Carta, J. A., Velázquez, S., & Cabrera, P. (2013). A review of measure-correlate-predict (MCP) methods
546 used to estimate long-term wind characteristics at a target site. *Renewable and Sustainable Energy*
547 *Reviews*, 27, 362–400. <https://doi.org/10.1016/j.rser.2013.07.004>

548 Devis, A., Van Lipzig, N. P. M., & Demuzere, M. (2018). Should future wind speed changes be taken into
549 account in wind farm development? *Environmental Research Letters*, 13(6).
550 <https://doi.org/10.1088/1748-9326/aabff7>



551 Draeger, C., Radić, V., White, R. H., & Tessema, M. A. (2024). Evaluation of reanalysis data and
552 dynamical downscaling for surface energy balance modeling at mountain glaciers in western
553 Canada. *Cryosphere*, 18(1), 17–42. <https://doi.org/10.5194/tc-18-17-2024>

554 Gentleman, R., & Poggi, J.-M. (2020). *Random Forests with R*. https://doi.org/10.1007/978-3-030-56485-8_3

556 Godoy, J. C., Cajo, R., Mesa Estrada, L., & Hamacher, T. (2025). Multi-criteria analysis for energy
557 planning in Ecuador: Enhancing decision-making through comprehensive evaluation. *Renewable
558 Energy*, 241. <https://doi.org/10.1016/j.renene.2024.122278>

559 Gualtieri, G. (2022). Analysing the uncertainties of reanalysis data used for wind resource assessment: A
560 critical review. *Renewable and Sustainable Energy Reviews*, 167.
561 <https://doi.org/10.1016/j.rser.2022.112741>

562 Hahmann, A. N., García-Santiago, O., & Peña, A. (2022). Current and future wind energy resources in the
563 North Sea according to CMIP6. *Wind Energy Science*, 7(6), 2373–2391.
564 <https://doi.org/10.5194/wes-7-2373-2022>

565 Hahmann, A. N., Sile, T., Witha, B., Davis, N. N., Dörenkämper, M., Ezber, Y., Garcíá-Bustamante, E.,
566 Fidel González-Rouco, J., Navarro, J., Olsen, B. T., & Söderberg, S. (2020). The making of the
567 New European Wind Atlas - Part 1: Model sensitivity. *Geoscientific Model Development*, 13(10),
568 5053–5078. <https://doi.org/10.5194/gmd-13-5053-2020>

569 Hallgren, C., Aird, J. A., Ivanell, S., Körnich, H., Vakkari, V., Barthelmie, R. J., Pryor, S. C., & Sahlée, E.
570 (2024). Machine learning methods to improve spatial predictions of coastal wind speed profiles and
571 low-level jets using single-level ERA5 data. *Wind Energy Science*, 9(4), 821–840.
572 <https://doi.org/10.5194/wes-9-821-2024>

573 Hersbach, H., Bell, B., Berrisford, P., Hirahara, S., Horányi, A., Muñoz-Sabater, J., Nicolas, J., Peubey,
574 C., Radu, R., Schepers, D., Simmons, A., Soci, C., Abdalla, S., Abellán, X., Balsamo, G., Bechtold,
575 P., Biavati, G., Bidlot, J., Bonavita, M., ... Thépaut, J. N. (2020). The ERA5 global reanalysis.
576 *Quarterly Journal of the Royal Meteorological Society*, 146(730), 1999–2049.
577 <https://doi.org/10.1002/qj.3803>

578 Houndekindo, F., & Ouarda, T. B. M. J. (2025a). LSTM and Transformer-based framework for bias
579 correction of ERA5 hourly wind speeds. *Energy*, 328. <https://doi.org/10.1016/j.energy.2025.136498>

580 Houndekindo, F., & Ouarda, T. B. M. J. (2025b). Machine learning and statistical approaches for wind
581 speed estimation at partially sampled and unsampled locations; review and open questions. *Energy
582 Conversion and Management*, 327. <https://doi.org/10.1016/j.enconman.2025.119555>

583 Hu, W., Scholz, Y., Yeligeti, M., Bremen, L. von, & Deng, Y. (2023). Downscaling ERA5 wind speed
584 data: a machine learning approach considering topographic influences. *Environmental Research
585 Letters*, 18(9). <https://doi.org/10.1088/1748-9326/aceb0a>

586 Jourdier, B. (2020). Evaluation of ERA5, MERRA-2, COSMO-REA6, NEWA and AROME to simulate
587 wind power production over France. *Advances in Science and Research*, 17, 63–77.
588 <https://doi.org/10.5194/asr-17-63-2020>

589 Khadka, A., Wagnon, P., Brun, F., Shrestha, D., Lejeune, Y., & Arnaud, Y. (2022). Evaluation of ERA5-
590 Land and HARv2 Reanalysis Data at High Elevation in the Upper Dudh Koshi Basin (Everest
591 Region, Nepal). *Journal of Applied Meteorology and Climatology*, 61(8), 931–954.
592 <https://doi.org/10.1175/JAMC-D-21-0091.1>

593 Kumar, R., Rutgersson, A., Asim, M., & Routray, A. (2025). Understanding Wind Characteristics Over
594 Different Terrains for Wind Turbine Deployment. *Meteorological Applications*, 32(4).
595 <https://doi.org/10.1002/met.70079>



596 Liu, B., Ma, X., Guo, J., Li, H., Jin, S., Ma, Y., & Gong, W. (2023). Estimating hub-height wind speed
597 based on a machine learning algorithm: Implications for wind energy assessment. *Atmospheric*
598 *Chemistry and Physics*, 23(5), 3181–3193. <https://doi.org/10.5194/acp-23-3181-2023>

599 Liu, B., Ma, X., Guo, J., Wen, R., Li, H., Jin, S., Ma, Y., Guo, X., & Gong, W. (2024). Extending the wind
600 profile beyond the surface layer by combining physical and machine learning approaches.
601 *Atmospheric Chemistry and Physics*, 24(7), 4047–4063. <https://doi.org/10.5194/acp-24-4047-2024>

602 López, G., Arboleya, P., Núñez, D., Freire, A., & López, D. (2023). Wind resource assessment and
603 influence of atmospheric stability on wind farm design using Computational Fluid Dynamics in the
604 Andes Mountains, Ecuador. *Energy Conversion and Management*, 284.
605 <https://doi.org/10.1016/j.enconman.2023.116972>

606 Martinez, A., & Iglesias, G. (2024). Climate change and wind energy potential in South America. *Science*
607 *of the Total Environment*, 957. <https://doi.org/10.1016/j.scitotenv.2024.177675>

608 Martinez, J. A., Junquas, C., Bozkurt, D., Viale, M., Fita, L., Trachte, K., Campozano, L., Arias, P. A.,
609 Boisier, J. P., Condom, T., Goubanova, K., Pabón-Caicedo, J. D., Poveda, G., Solman, S. A.,
610 Sörensson, A. A., & Espinoza, J. C. (2024). Recent progress in atmospheric modeling over the
611 Andes – part I: review of atmospheric processes. *Frontiers in Earth Science*, 12.
612 <https://doi.org/10.3389/feart.2024.1427783>

613 McKenna, R., Pfenninger, S., Heinrichs, H., Schmidt, J., Staffell, I., Bauer, C., Gruber, K., Hahmann, A.
614 N., Jansen, M., Klingler, M., Landwehr, N., Larsén, X. G., Lilliestam, J., Pickering, B., Robinius,
615 M., Tröndle, T., Turkovska, O., Wehrle, S., Weinand, J. M., & Wohland, J. (2022). High-resolution
616 large-scale onshore wind energy assessments: A review of potential definitions, methodologies and
617 future research needs. *Renewable Energy*, 182, 659–684.
618 <https://doi.org/10.1016/j.renene.2021.10.027>

619 MEASNET. (2022). *Evaluation of Site-Specific Wind Conditions*.

620 Olauson, J. (2018). ERA5: The new champion of wind power modelling? *Renewable Energy*, 126, 322–
621 331. <https://doi.org/10.1016/j.renene.2018.03.056>

622 Pauscher, L., Geiger, D., Yuan, D., Bär, F., Good, G., Spangehl, T., Kaspar, F., Weber, H., & Callies, D.
623 (2024, September). An evaluation and comparison of wind speeds from different reanalysis models
624 in the context of wind energy – the influence of topography. *EMS Annual Meeting 2024*.
625 <https://doi.org/10.5194/ems2024-957>

626 Ramon, J., Lledó, L., Torralba, V., Soret, A., & Doblas-Reyes, F. J. (2019). What global reanalysis best
627 represents near-surface winds? *Quarterly Journal of the Royal Meteorological Society*, 145(724),
628 3236–3251. <https://doi.org/10.1002/qj.3616>

629 Rouholahnejad, F., & Gottschall, J. (2025). Characterization of local wind profiles: a random forest
630 approach for enhanced wind profile extrapolation. *Wind Energy Science*, 10(1), 143–159.
631 <https://doi.org/10.5194/wes-10-143-2025>

632 Schwegmann, S., Faulhaber, J., Pfaffel, S., Yu, Z., Dörenkämper, M., Kersting, K., & Gottschall, J.
633 (2023). Enabling Virtual Met Masts for wind energy applications through machine learning-
634 methods. *Energy and AI*, 11. <https://doi.org/10.1016/j.egyai.2022.100209>

635 Tapia, M., Heinemann, D., & Zondervan, E. (2026). Too many eggs in one basket: On the vulnerability of
636 the Ecuadorian power system and the need for a more sustainable and resilient strategy. *Energy*
637 *Policy*, 209. <https://doi.org/10.1016/j.enpol.2025.114951>

638 Watson, S. (2023). *Handbook of Wind Resource Assessment*. John Wiley & Sons Inc.

639